Characterizing Temporal SNR Variation in 802.11 Networks

Ratul K. Guha and Saswati Sarkar

***Abstract*— The analysis and design of wireless MAC protocols, coding schemes and transmission algorithms can significantly benefit from an understanding of the channel quality variation. We attempt to represent channel quality variation using a finite state birth-death Markov model. We outline a method to compute the parameters of the model based on measured traces obtained using common wireless chipsets. Using this Markov chain, we evaluate the performance statistically based on the channel quality, long term correlations and burst length distributions. Such a model performs significantly better than a traditional two-state Markov chain in characterizing 802.11 networks while maintaining the simplicity of a birth-death model. We interpret the variation of the model parameters across different locations and different times. A finite state stationary model is amenable to analysis and can substantially benefit the design of efficient algorithms and make simulations for wireless network protocols faster.**

I. Introduction

Wireless networks are being rapidly deployed all over the world. In the U.S several companies like Boingo, Cometa and T-mobile are deploying nationwide IEEE 802.11b based wireless local area networks. This large scale deployment has motivated the research for design of better wireless systems. An important step in that direction is to characterize the Signal to Noise ratio (SNR) in these networks. SNR determines several important attributes like packet loss that affects network performance and design at all levels of the network stack. The challenge in this characterization is that the SNR process is a result of both interference due to simultaneous transmission of multiple users and vagaries of radio wave propagation. Several resource allocation policies in wireless local area networks require this characterization in predicting channel qualities. Also, distribution of error bursts and error-free bursts can be obtained from the characterizations for the temporal variations of the SNR as the packet error processes depend on the SNR. Thus, the SNR is a more fundamental attribute of the system. Our goal is to approximately characterize the channel behavior with a stationary process that is conducive to analysis and simulation for large systems. Towards this end, we characterize the SNR variations on a packet time-scale. Furthermore, we use a birth-death Markov model with finite number of states for characterizing the SNR variations. The advantage of birth-death models is that they are simple and analytically tractable.

Significant research has been directed towards modeling fading channels with Rayleigh distributed signal to noise ratio [16], [21]. But, it is not clear that the same techniques would apply for modeling IEEE 802.11 channels as these experience both interference and frequency-selective fading. Most of the research for modeling IEEE 802.11 systems have been directed towards modeling protocol behavior [4], [12] or obtaining distributions for error bursts and sequences of error free transmissions using traces of packet losses [1], [15], [18]. Much attention has been devoted to the two-state Gilbert/Eliott model [6], [7] owing to its analytical simplicity. However, the two-state models have severe limitations. This has been observed by authors in [19], who use a bipartite model for characterizing packet losses, whereas [10] uses HMM models for modelling losses. Regression and learning-based models have also been proposed for link quality estimation [20], [11] These models are non-stationary and as a result are more suitable for simulation and trace generation rather than analysis. Our goal on the other hand is to present a stationary birth-death model that is simple and rapid for computation without compromising the model performance significantly.

We characterize the temporal variation of the SNRs of IEEE 802.11 channels and explain several attributes of the wireless systems using the characterization. Note that the variation of the SNR will be a non-stationary process as this is effected by the traffic which is not a stationary process. Hence no stationary model will provide an exact statistical match. However, non-stationary models exclude many analytical techniques, and simulations using non-stationary models can take a significant amount of time

Ratul K. Guha and Saswati Sarkar are with the University of Pennsylvania. Emails: rguha@seas.upenn.edu and swati@ee.upenn.edu.
Parts of this paper have appeared at IEEE WCNC 2006.

especially in large-scale systems.

Drawing from the literature known for fading channels, we propose a framework for determining the parameters of the birth-death Markov model for IEEE 802.11 channels (Section II). We discuss two forms of measurements, namely passive and active. Passive measurements involve collecting traces from existing network traffic. Active measurements involve sending probe packets. Active measurements are often useful since probe packets can be generated periodically to update the parameters of the model. However, active measurement has the disadvantage of affecting the very channel that is being measured. This happens because of the interference generated by the probe traffic. Passive measurement on the other hand require longer times scales for trace collection. However various user characteristics such as mobility and other non-stationary behavior of the users can be studied using passive measurements. In this work we primarily focus on passive measurements.

In Section III, we discuss the passive measurement setup and classify broadly the environments in which we collected the traces. We subsequently validate our model using statistical comparison with passively collected SNR traces over Wi-Fi channels (Section IV and V). This validation demonstrates that a simple birth-death Markov model characterizes the SNR variations in IEEE 802.11 channels reasonably accurately. In SectionVI, we evaluate the effectiveness of active measurements and compare the model with that obtained from the passive measurements. We notice that active measurements can be leveraged to construct the channel model without significantly disrupting the network. Finally, using our model we investigate and explain several attributes of the wireless systems like statistics of error bursts in Section VII. For example, in [1] and [19] the authors conclude that the two-state Gilbert-Eliot model is not suitable for characterizing packet losses, whereas the authors in [10] claim that two-state models are sufficient for capturing the packet loss process but not the bit losses. Using our characterization, we explain the difference between these conclusions and provide several general guidelines about the characteristics of IEEE 802.11 channels. We conclude in Section VIII.

II. Modeling the 802.11 Channel

We first outline the 802.11 frame format and describe how to evaluate the packet error probabilities based on bit probabilities (Section II-A). The bit error probabilities are functions of the Signal to Interference and Noise ratio. We will then present a framework for modelling the SNR using a finite state Markov model and present a methodology for computing the parameters of the model based on measured traces in Section II-B. Henceforth the ratio of signal power to the interference and ambient RF power is referred to as SNR.

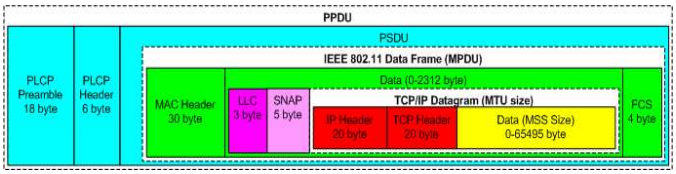

Fig. 1. 802.11 Frame Format

A. 802.11 Physical Layer

The IEEE 802.11b physical layer (PHY) is an extension of the original Direct Sequence Spread Spectrum(DSSS) PHY. It operates in the 2.4GHz ISM band and provides PHY data rates of 5.5 and 11Mbps in addition to the 1 and 2Mbps rates supported by the original DSSS. The 1Mbps rate is based on the Binary Phase Shift Keying(BPSK) and the 2Mbps rate is based on the Quadrature Phase Shift Keying(QPSK) modulation. They are encoded using DSSS based on the 11-bit Barker chipping sequence that results in a signal spread over a wider bandwidth at a reduced RF power. For 5.5 and 11Mbps the IEEE 802.11b uses the Complementary Code Keying(CCK) modulation scheme which is a variation of the M-ary Orthogonal Keying Modulation. For each word, the 5.5Mbps rate encodes 4 bits while the 11Mbps encodes 8 bits. The spreading maintains the same chipping rate and spectrum shape as the original 802.11 DSSS and hence occupies the same channel bandwidth. There are 11 channels and each channel occupies 22MHz around the center frequency. This allows for 3 non-overlapping channels(1, 6 and 11) in the band.

The IEEE 802.11b frame format is shown in Fig.1. When a higher layer frame also called the Medium Access Control (MAC) Service Data Unit (MSDU) arrives at the MAC layer it is encapsulated in a MAC Protocol Data Unit (MPDU) by adding a MAC header and Frame Control Sequence(FCS). The MAC header is 24 bytes and the FCS is 4 bytes. We now evaluate the packet success probability. The MAC Protocol Data Unit (MPDU) is passed down to the PHY layer which attaches a 6 Byte Physical Layer Convergence Protocol (PLCP) header and a 18 Byte preamble. The PLCP header and preamble is transmitted at 1 Mbps BPSK. Suppose that an L byte MPDU is to be transmitted using Physical layer rate r, where r can be 1, 2, 5.5 and 11 Mbps. A packet is successful if both the PLCP header and the MPDU is received correctly. Hence, the success probability of a packet $P_r(L)$ with an L byte

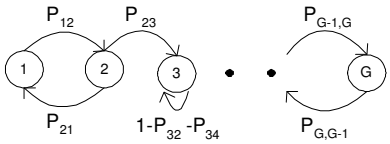

Fig. 3. Channel Model.

long MPDU can be written as

$$P_r(L) = P_1(24)P_r^{\text{MPDU}}(L). \quad (1)$$

where

$$P_1(24) = \prod_{i=1}^{192} P_1^{b,i} \text{ and } P_r^{\text{MPDU}}(L) = \prod_{i=1}^{8L} P_r^{b,i}. \quad (2)$$

where $P_r^{b,i}$ is the bit-success probability seen by the ith bit when the transmission occurs at rate r. The equations assume conditional independence of the bit success probabilities given the SNR at a bit. $P_r^{b,i}$ can be obtained from the actual chipset SNR-BER curves in Fig.2.

Typical off the shelf wireless chipsets [2], [9] report SNR measurements in terms of RSSI value once per packet. Using the available data, we now present the procedure to evaluate the parameters of the Markov chain based on measurements that can be obtained from common hardware.

B. Finite State Model for SNR Variation

We next present a methodology to model SNR variations using a finite state Markov chain with state space $\mathcal{S} = s_1, s_2 \dots s_G$. Each of the G states corresponds to a certain channel quality and an associated packet success probability. G is a parameter and needs to be fixed. We will later discuss how to select an appropriate value for G. We will obtain the transition rates and the steady state probabilities for the Markov chain. We assume that the transitions happen between the adjacent states. Such a choice is intuitive because normally the channel transitions are not abrupt but continuous and then, if the SNR intervals are chosen with a high granularity then transitions between non-adjacent states can be avoided. This allows us to use birth-death models which are amenable to analysis. We adapt the methodology used for fading channels in [16], [21]. In [16], the model parameters are analytically obtained based on a fading model. The main difference between [16] and our paper is that the authors in [16] derive the values of model parameters from fading models, whereas we compute the values of the model parameters from measurement traces. The reason we adopt this approach is that in our case the reception quality is determined both by fading and interference, and models used for fading may not be appropriate for interference. We will demonstrate that the framework for fading channels is a good model for Wi-Fi channels. The SNR trace i.e. the SNR recording for every received packet is to be partitioned into G states based on time duration. A received packet is said to face state s_k if the SNR values that the bits comprising the packet face are in the range $[\Gamma_k, \Gamma_{k+1})$. We will compute the SNR thresholds $\vec{\Gamma} = [\Gamma_1, \dots \Gamma_{G+1}]$, $\Gamma_1 = 0$, $\Gamma_{G+1} = \infty$ and $\Gamma_k < \Gamma_{k+1}$ to partition the SNR process. Let P_{ij} and π_i be the state transition probability and the steady-state probability respectively. Since the transitions happen between the adjacent states, hence $P_{k,i} = 0$ for $|k - i| > 1$.

Let $N(\Gamma)$ be the level crossing rate of the SNR process in the positive direction only (or in the negative direction only). Essentially, this is the number of times the SNR crosses a level Γ in a particular direction divided by the total time.

Let $\bar{\tau_k}$ be the average duration of the SNR interval $[\Gamma_k, \Gamma_{k+1})$. This is the average time the SNR process remains continuously between Γ_k and Γ_{k+1} over a measurement interval T. For simplicity of exposition we assume a fixed packet size with transmission time T_p in order to outline the procedure. We require that the average duration of a state is some constant times the packet transmission time T_p, i.e. $\bar{\tau_k} = c_k T_p$. We let $c_k = c \; \forall \; k$. In other words each state has the same average duration. We justify such an assumption. The states in which the system spends more time are more important for characterizing the system. Thus these states should be represented with a higher SNR granularity. This can be achieved by subdividing these states such that the time duration assigned to each substate is reduced, which in turn means that all states have equal duration.

The steady state probability π_i is the total time during which the SNR level is between Γ_i and Γ_{i+1} divided by the total time T i.e. $\pi_i = \text{Prob}(\Gamma_i \leq \Gamma < \Gamma_{i+1})$. Note that π_i can be evaluated from the trace if Γ_i and Γ_{i+1} are known. $\bar{\tau_k}$ is then the ratio of the total time the signal remains between Γ_k and Γ_{k+1} and the number of these signal segments. The number of such signal segments differs from $(N(\Gamma_k) + N(\Gamma_{k+1}))T$ by at most 1 since the number of upcrossings and downcrossings can differ by 1 and this error becomes insignificant for large traces.

Hence

$$\bar{\tau_k} = \frac{\pi_k T}{(N(\Gamma_k) + N(\Gamma_{k+1}))T} = \frac{\pi_k}{N(\Gamma_k) + N(\Gamma_{k+1})}.$$

Thus we have

$$cT_p = \frac{\pi_k}{N(\Gamma_k) + N(\Gamma_{k+1})} \text{ for } k \in [1 \dots G]. \quad (3)$$

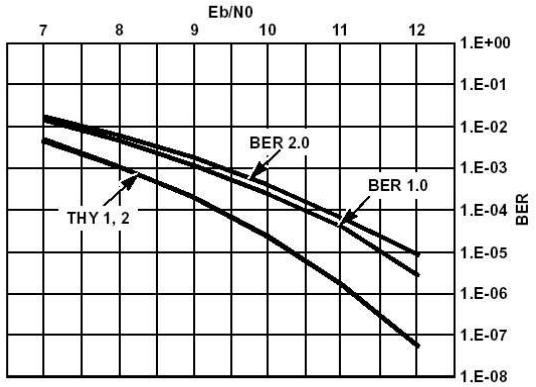

(a) SNR-BER for PSK Modes.

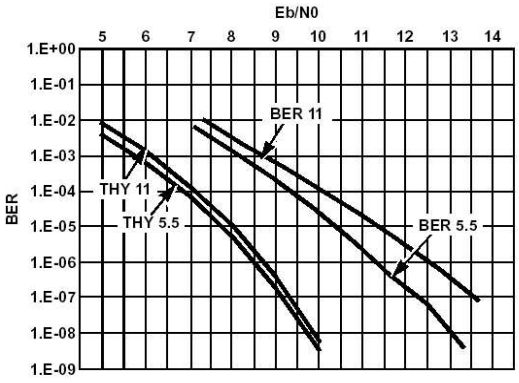

(b) SNR-BER for CCK Modes.

Fig. 2. SNR-BER curves. The curved marked BER are the actual curves for the chipset and curves marked THY are the theoretically obtained curves.

We require our solution to satisfy G equations in (3). The variables are c and $\vec{\Gamma} = [\Gamma_1, \ldots \Gamma_{G+1}]$ with $\Gamma_1 = 0$ and $\Gamma_{G+1} = \infty$. Hence there are G variables. One way to solve this system is to take an initial guess for c and subsequent iteration. $\Gamma_2, \Gamma_3 \ldots \Gamma_G$ can be successively obtained using $k = 1, 2 \ldots G$ respectively in (3). Note that $N(\Gamma)$ can be evaluated from the trace for every Γ.

Once $\vec{\Gamma}$ is determined, the transition probabilities can be computed as the ratio of the level crossing rate and the average number of packets staying in that state, i.e.

$$P_{k,k+1} = \frac{N(\Gamma_{k+1})T_p}{\pi_k}, k = 1, 2, \ldots, G-1$$

and

$$P_{k,k-1} = \frac{N(\Gamma_k)T_p}{\pi_k}, k = 2, \ldots, G$$

Using the above transition probabilities and (3), the memory of a state i.e. $1 - P_{k,k+1} - P_{k,k-1}$ is $1 - 1/c$.

We describe the method to obtain the average success probabilities for the states. The SNR-BER mappings are obtained from the characteristics in Fig.2 [9]. Let $P(x)$ be the packet success probability for SNR level x. Also let $n(x)$ be the fraction of time SNR level x is observed in the SNR trace. Then the average probability of success conditioned on state s_k, $\alpha(k) = \frac{\sum_{x=\Gamma_k}^{\Gamma_{k+1}} P(x)n(x)}{\pi_k}$ where the summation is over the discrete SNR values that comprise state s_k.

Next we present our measurement setup and trace collection scenarios. We will use the data from the trace recordings and evaluate the Markov chain based on the preceding discussion.

III. Measurement Setup and Trace Collection

We now describe our measurement setup and the trace collection procedure. Our hardware comprises of two Dell Lattitude X200 laptops with internal Agere cards and a PCMCIA slot. The wireless NICs are Cisco CB21AG-AK9 and the RFgrabber [17] with an Intersil chipset. A host Windows XP workstation running Airopeek NX [17] connects to the RFgrabber to store packets. We use the Airopeek NX [17] packet analyzer for measurement purposes[1]. We capture all IEEE 802.11 management packets (Beacons), data packets (TCP, UDP) and control packets (ACKS) which comprise 98% of the traffic. For each packet from the Access Point (AP), the Airopeek NX trace records the time stamp, the signal strength, the channel number, the noise level, the packet size, the transmission speed, the protocol and the packet error flag. Erroneous Packets are flagged according to radio error, decryption error or a CRC error.

We conduct our measurement in different kinds of Wi-Fi environment and at different time instants to obtain a variety of possible channel characteristics. We broadly describe the different settings that we believe are representative for recording the data.

1) Locations close to the AP with few users e.g. classrooms
2) Locations close to the AP with large number of users e.g. hotspots, conference rooms etc.
3) Locations distant from the AP in relatively less crowded areas e.g. parks
4) Locations distant from the AP in crowded areas.

[1]We use Network Stumbler(NS) [14] for cross-verification of signal levels. NS is an active scanner that scans all 11 channels sending probe requests.

In the first case the channel is referred to as *good*. Here, the signal strengths are high and the error probabilities are small($<3\%$) with SNR $>$25dB. The second and the third cases are what we refer to as *intermediate* channels. In the second case the interference is higher than the first. For the third case the signal strength is lower than the first. As compared to the first case, both the second and the third case experience lower SNR 10-20dB and higher packet error with error rates 5-10%. The fourth case is referred to as a *poor* channel with signal strength lower and the interference higher than the first. Here the packet error rates are as high as 50% with SNR $<$10dB. The first three cases are more likely to arise in practice, but we consider all cases for completeness.

The trace recording is carried out for a duration of 20 minutes at 2 hour interval for a period of seven days. We observe that a majority of the users have short session times that are less than 10 minutes and the duration of portions when the usage pattern remains similar are approximately around 6-7 minutes. This observation is consistent with reports in [3]. We continuously record data for 20 minutes at any given time.

Next we evaluate the effectiveness of the finite state Markov model for the temporal SNR variations.

IV. Testing of the Model Based on Traces

We proceed to evaluate the efficacy of the finite state Markov model. We first evaluate the performance of the model in terms of tracking the SNR obtained directly from the measurement. We also evaluate the model in terms of capturing statistics relevant from the perspective of higher layer wireless protocols. The statistics of interest typically comprise the moments of the error free and the error burst lengths. Also long term correlation of the packet error process is of interest in predicting the future channel behavior. Since different performance attributes are of interest for different systems, we evaluate our model based on several different factors: (a) the values of the maximum and the average differences between the model parameters obtained from our methodology, and those obtained from the model traces (Section IV-A) (b) statistical divergence between the distribution of the channel states obtained from our model and the distribution obtained directly from the traces and (Section IV-A) (c) the differences in performance attributes (e.g., error burst lengths, error-free burst lengths, etc.) (Section IV-B, IV-C, IV-D). We make our conclusions based on all of the above. We specify the values of the maximum and average differences between the model parameters so that the system designers can decide whether this difference leads to the accuracy they desire for the performance attribute important to them.

We now describe the statistical measure that we use to quantify the performance of the model.

Let $p(x)$ and $q(x)$ be two probability mass functions defined over a common set $\mathcal{X}$. We now describe a commonly used statistical measure that quantifies the 'distance' or the relative entropy between two probability distributions. This comprises a general measure and allows us to compare the statistics of all orders for two distributions.

The *Kullback-Leibler Divergence*(KLD) [5] is defined as

$$D(p(x)||q(x)) = \sum_{x\in\mathcal{X}} p(x) log \frac{p(x)}{q(x)}.$$

The KLD is zero when the distributions are identical and strictly positive otherwise. The KLD is a measure of the 'distance' between two distributions. However the measure is not symmetric and does not satisfy the triangle inequality. The definition of the divergence measure carries a bias. This discrimination is larger for random variables with higher entropy. The entropy $H(p(X))$ of the random variable X with distribution $p(X)$ is $\sum_{x\in\mathcal{X}} p(x) log \frac{1}{p(x)}$. Hence to evaluate the model it is important to weigh in the entropy of the source which could be large. Hence we use the normalized Kullback-Leibler divergence [13] NKLD.

$$NKLD(p(x)||q(x)) = \frac{D(p(x)||q(x))}{H(p(X))}$$

Since the order of the distributions is important we consider the distributions derived from the measured trace as $p(x)$ and those derived from the Markov model as $q(x)$ in the subsequent discussion.

A. SNR Variation

To test the model, we first examine the SNR values from the trace at equal intervals of time for the purpose of developing the Markov chain. The interval corresponds to transmission times of data packets which are longer than the control and management packets. We used the transmission time for a 1000 Byte packet(0.73ms) as the interval. The computation time for model generation depends on the length of the available trace. In our case generating the model from a 7 minutes trace required approximately 15 seconds on a 750Mhz laptop with 256MB RAM. From the Markov chain we generate an artificial channel trace for the SNR variation.

The difference between the SNR values from the actual trace and the trace obtained from the channel model is examined. The root mean square percentage difference is observed to be less than 4%. We also evaluate the NKLD

between the probability mass function of the SNR obtained from the measured trace and the Markov model. The probability mass function defines the probability of the SNR lying in certain intervals. The setup is shown in Fig.4. The NKLD measure is plotted for three kinds of channels in Fig.5 as the number of states increases. The low value of the NKLD measure signifies the proximity of the two distributions. To get a feel of how rapidly the NKLD increases as the distributions become separate, we use a naive channel model and evaluate its performance. We partition the entire SNR range into G states of equal SNR length that are equiprobable. The NKLD value will increases to more than 0.7 for all values of G. On the other hand, using a time varying distribution using phase type models reduces the NKLD to below 0.009. This improvement comes at the expense of using a non-stationary model.

We notice a small value of the divergence between the actual SNR trace and the trace obtained from the channel model that does not decrease further with the increase in the number of states. We first investigate whether this divergence is lower if the channel is modelled by a more general Markov chain. For this, we use a general Markov model to characterize the SNR process where the transitions can occur between any two states. The state space is defined in a way similar to the birth-death model. The transition probability from a state X to any other state Y is obtained from the SNR trace by calculating the ratio of the total number of transitions from X to Y and the total number of transitions from state X. The total number of transitions from state X include all the transitions out of X and those that go back to itself. The performance using this model is shown in Fig.6. We notice that a Markov model with arbitrary transitions does not yield any significant improvement in the model performance Fig.6. The intuition is that the model represents states with a high time granularity and within this time scale SNR values change gradually. Hence transition to far away states occur rarely. Hence, among Markov models a birth-death model is good enough.

We believe that the reason for the residual divergence is that we use a irreducible, aperiodic, finite state Markov chain to model the SNR process. Such a model has a stationary distribution. However, the SNR process is expected to be non-stationary due to physical reasons such as node mobility, traffic variations, fading etc. We establish the non-stationarity of the process using a statistical analysis of the trace. The stationarity of the trace is investigated using a derived time lag. In Fig.7 we plot the coefficient of correlation as the time lag W is increased i.e. we select vectors from the trace shifted by W. We note that

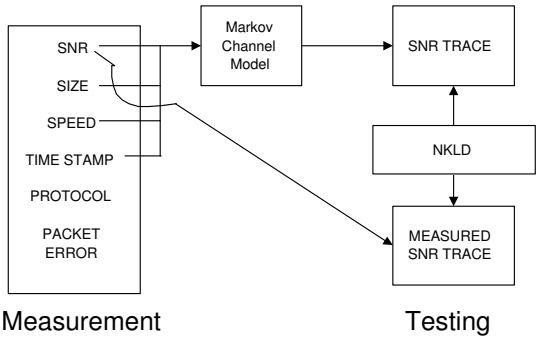

Fig. 4. Measurement and Testing Setup for SNR Trace.

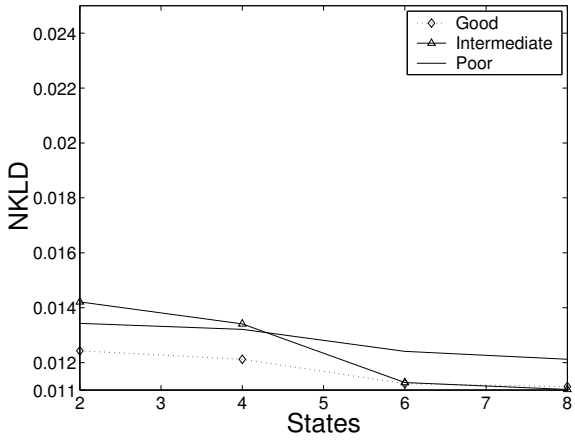

Fig. 5. SNR Distribution with a Birth-death Markov chain.

for $W > 800$ the correlation goes down to zero ensuring we have a sufficiently large lag such that the transients have died down. Hence, for determining mean we use a time lag of 1000. We note that the mean over time lags of 1000 plotted in Fig.8 changes by almost 10% with time indicating non-stationarity. This non-stationary behavior cannot be captured by stationary ergodic models resulting in the observed divergence. Nevertheless, the residual divergence is small with a stationary ergodic birth-death model, which unlike non-stationary models is amenable to analysis.

We also develop the Markov chain based on SNR information obtained from 802.11 beacon packets in Fig.9. Although the beacon packets are relatively infrequent(100ms), the Markov chain approximates the channel behavior well even in this case. Furthermore, in subsections IV-B and IV-C, we also demonstrate that the statistical characteristics of empirical observations for several attributes like burst length processes match those obtained from the birth-death model, which corroborates our conclusion that a birth-death Markov chain models the SNR process reasonably well.

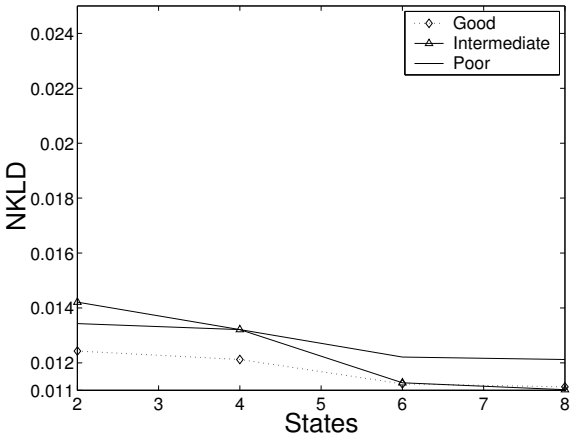

Fig. 6. SNR Distribution with Markov chain having arbitrary transitions.

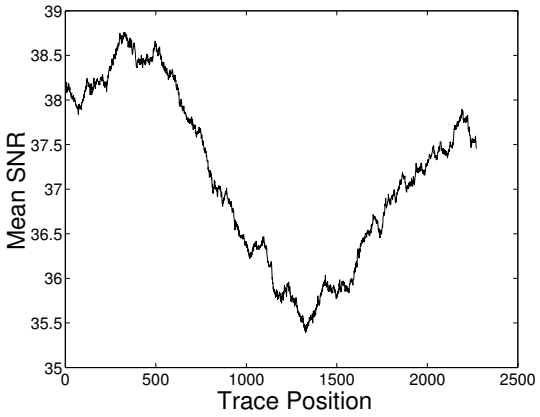

Fig. 8. Mean values over different windows. The Y-axis value corresponding to X-axis point k, denotes the mean from position k to $k + 1000$ in the trace.

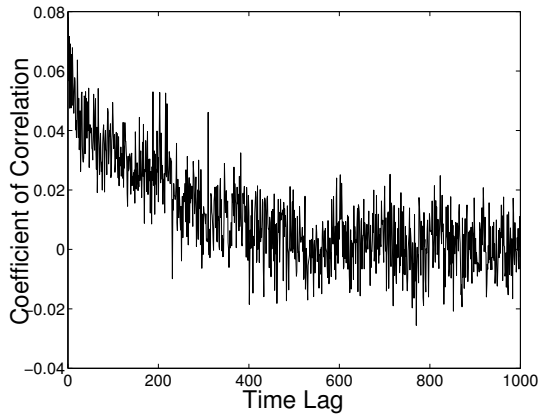

Fig. 7. Coefficient of correlation with time lag.

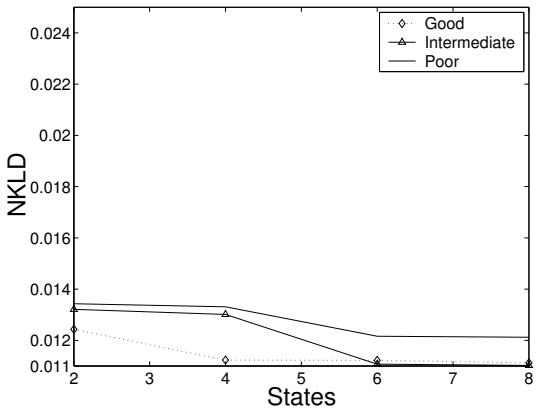

Fig. 9. Channel model using Beacon packets.

B. Packet Error model and SNR sampling

We now study various attributes of the system for e.g. the packet error process that can be derived from the SNR process. Towards this, we first study and evaluate the effect of fundamental measurement limitations. We will then evaluate the efficacy of the SNR measurements in characterizing the packet errors.

We proceed to evaluate the effect of two fundamental measurement limitations imposed by software and hardware. Firstly, common Wi-Fi hardware record the signal strengths and the noise levels once per packet. However any of the intermediate bits of a packet can get corrupted and predicted packet errors based on reported SNR could be significantly different from actual packet errors. We will investigate whether the memory in the channel is high enough for an SNR interpolation between packet boundaries to be useful.

Secondly, the SNR-BER characteristics reported by card manufacturers as as shown in Fig.2 are obtained under Additive white gaussian noise(AWGN) environment which might not be the case in practice. Also the RSSI values i.e. the units in which the cards report the signal levels and signal values(dBm) do not have a one-to-one correspondence. For example, in Cisco cards, an RSSI of both 63 and 64 correspond to -44dBm. These factors can result in discrepancies between the calculated packet errors based on SNR measurements and the observed packet error process. We will check how closely the packet error model we use, mimics the behavior of the actual channel. Specifically we would be focussing on the distributions of the packet error burst lengths and error free lengths. The random variable depicting the error free length I denotes the number of good packets received between error packets. The error burst length B is the length of consecutive packet errors. Packet error bursts are responsible for degrading the throughput in wireless transmission because they are harder to recover from. Isolated packet errors are mostly recovered from, using error correcting and redundancy coding schemes.

We now present an outline of the procedure. From the per packet SNR values of the captured packets a first order interpolated SNR sequence for each bit of the packet

is generated. The hypothesis is that the interpolated SNR values are those that bits of the packets face. We then use the SNR-BER curves [9] as shown in Fig.2 to get the bit error probability for each bit of the packet. This results in a packet error trace that is obtained after SNR interpolation and SNR-BER conversion. This trace is compared with the actual packet error trace obtained from the error flags. For this comparison, we plot the NKLD in Fig.10. The low value of the divergence validates such a SNR to packet error conversion procedure.

C. Burst Length Process

Now we study the burst length process that can be derived from the channel model. Using (1) and Fig.2, the SNR values yield the packet success probabilities that results in a packet loss trace which we refer to as the Markov generated packet trace. The setup is shown in Fig.11.

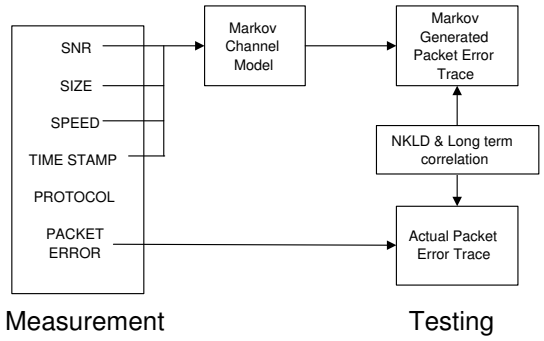

Fig. 11. Measurement and Testing Setup for Packet Loss trace.

We obtain the probability mass function of I and B from the observed packet error trace. Again we compute the probability mass function of I and B from the Markov generated packet error trace. The setup is shown in Fig.11.

We compare the NKLD between the actual trace and the Markov trace. Specifically, we observe the variation in the NKLD as the number of states in the model is increased. In Fig.12(a), we observe a very slight reduction in the NKLD measure as the number of states is increased. This is because even though the variation in SNR is significant, the actual SNR values are high so that the packet success rate is high. However for intermediate and poor channel the SNR variation is in a range where the packet success probabilities vary. It is in these regions that we need higher granularity to define the state space of the SNR process.

The NKLD measure in Fig.12 now includes the discrepancy accrued due to SNR trace to packet error trace conversion as well as the model for the SNR variation. We attempt to identify the contribution of each of these two factors towards the NKLD. We note the packet error trace directly obtained from SNR values and the actual packet errors observed in Fig.10. The NKLD values do not increase significantly in Fig.12 when compared with Fig.10. Hence, this indicates that it is the SNR-packet error trace evaluation that results in the discrepancy rather than the model for the SNR variation.

D. Long Term Correlation

We study the performance of the Markov model in terms of capturing long term correlation i.e. the conditional probability that packet $n + k$ is in error, given that packet n is in error. In Fig.13 we plot the performance of the Markov model in tracking long term correlation. As seen in the plot, a Markov chain with 8 states performs significantly better than one with 2 states. However both models are not able to capture the long term correlation with a discrepancy of more than 7% which occurs because the actual trace is non-stationary and no stationary model can capture the variations in a long run. The empirical average does not deviate from the actual average by more than 2% with 95% confidence.

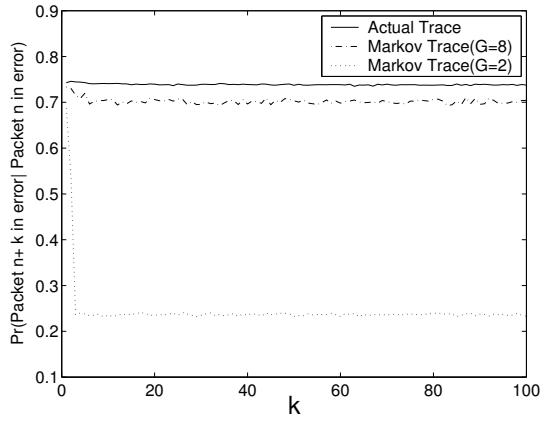

Fig. 13. Conditional probability that packet $n + k$ is in error given that packet n is in error.

We now present evaluations for studying the performance of the channel model on traces collected from traffic sent by the users.

V. Testing of the Model Based on User Traces

We proceed to evaluate the efficacy of the finite state Markov model in modelling the reverse channel i.e. the users to the AP. So far the study have been carried out based on traces collected from the traffic sent by the AP. The forward and the reverse channels are known to be asymmetric. We now perform a study when user traces are collected at the AP to investigate the behavior of the reverse channel. Here packets received from a specific user MAC address are examined for evaluation purposes. We

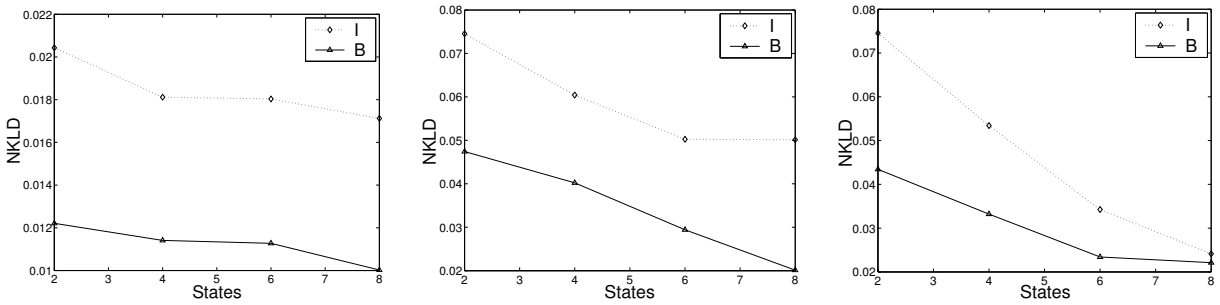

(a) Good channel. (b) Poor Channel. (c) Intermediate channel.

Fig. 10. NKLD measure for burst lengths from actual error trace and the packet trace from the SNR for different kinds of channels.

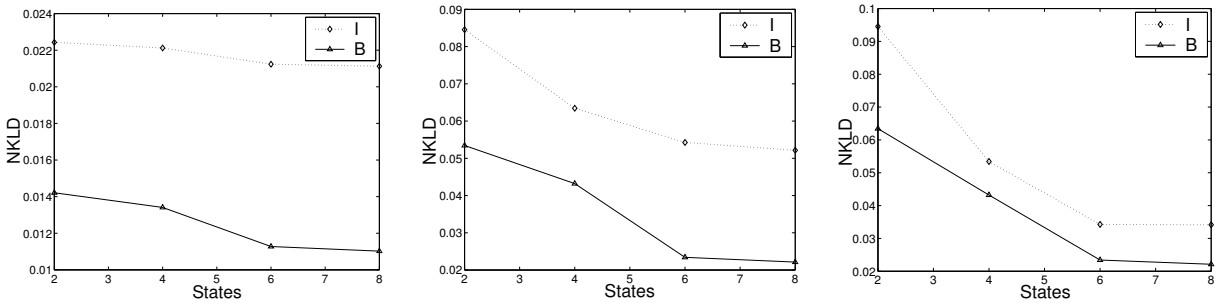

(a) Good channel. (b) Poor Channel. (c) Intermediate channel.

Fig. 12. NKLD measure for burst lengths from actual and Markov generated packet trace for different kinds of channels.

demonstrate that similar conclusions hold when user traffic is collected as compared to when the AP traffic is collected. As expected, the parameters of the model obtained in this case are different from those for traffic from the AP. Nevertheless, the statistical match between the model and the empirical traces is still satisfactory, and other general conclusions are the same as well.

The difference between the SNR values from the actual trace and the trace obtained from the channel model is now examined. The root mean square percentage difference is observed to be less than 4%. We also evaluate the NKLD between the probability mass function of the SNR obtained from the measured trace and the Markov model. The probability mass function defines the probability of the SNR lying in certain intervals. The setup is shown in Fig.4. The NKLD measure is plotted for three kinds of channels in Fig.14 as the number of states increases. The low value of the NKLD measure signifies the proximity of the two distributions.

Using a Markov model with arbitrary transitions as shown in Fig.15 does not yield any significant improvement in the model performance. Here unlike in Section IV, we do not perform error burst testing. This is because the SNR-BER curves of the AP chipset and the AP antenna characteristics are not available. We now present the evaluations.

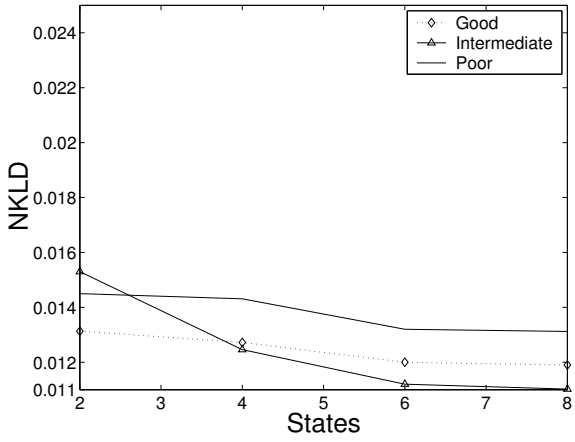

Fig. 14. SNR Distribution.

We note that network events such as load variation and mobility influence both the forward (to the AP) and the reverse (from the AP) channel. The channel models obtained for the forward and the reverse channel have different parameters. However the effectiveness of the corre-

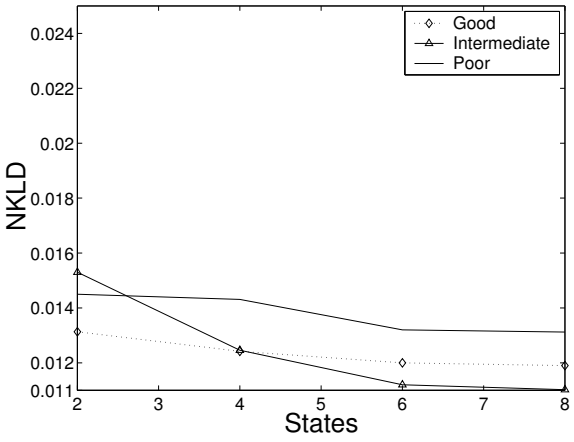

Fig. 15. SNR Distribution with Markov chain having arbitrary transitions.

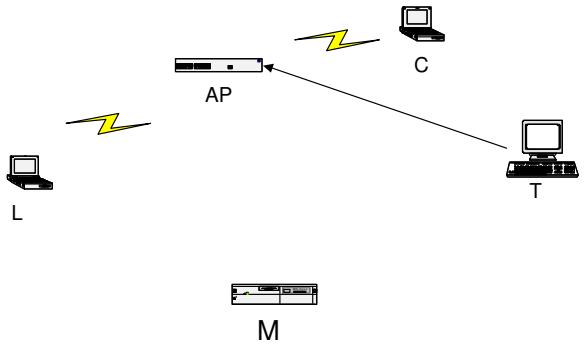

Fig. 16. The client C is associated with the Access Point AP and receiving UDP traffic. The laptop L is in promiscuous mode associated with AP. The wired workstation T is sending UDP traffic to L. M is in monitor mode listening to all the wireless traffic.

sponding Markov models in terms of the divergence measure is not different.

VI. Probe Based Measurement

In previous sections we have focussed on traces collected as a result of passive monitoring of the network. Such measurements require monitoring the network on a large time scale due to highly varying nature of the traffic. Additionally the traffic rate can be very low in order for the collected trace to be meaningful in capturing the channel statistics. In this section, we investigate the behavior of our model when active measurements are used for trace collection. Here probe traffic is generated in different ways and corresponding traces are collected. Although active measurements influence the channel due to the interference generated by the probe traffic, such measurements can be very useful for quick channel evaluation owing to its adaptability.

The difference between the active and the passive measurements will result because of the presence of a probe traffic in the active measurements. To investigate the effect of the probe traffic and how they influence the Markov channel model, we consider three scenarios. The first scenario is an isolated setup to perform the measurement under controlled conditions. Thereafter we consider two setups to collect traces in the presence of traffic from other user.

The isolated setup is shown in Fig.16. The wired workstation T uses MGEN to generate UDP traffic destined for L. The client C is receiving UDP traffic from the AP at the rate of 2 Mbps (500 packets per second with 512B packets).

We first observe the influence of the packet rate on T-AP-L on the traffic from AP-C. As the rate on T-AP-L is increased there is an increase in the inter packet time observed for the traffic from AP to C Fig.17. However the throughput suffers only when the total packet load exceeds a certain threshold as seen in Fig.18. We want the probe rate to be sufficiently low so as not to influence the existing user sessions.

We then develop the model based on the packet trace from link AP-L. The packet transmission time i.e. T_p is the same irrespective of the number of packets that are generated on the link T-AP-L since the transmission rate is 11 Mbps. We investigate the sensitivity of the Markov model when the probe traffic rate is changed. The investigation is essential as if the model parameters were to substantially change with change in the probe rate then the probe rate ought to be determined carefully. We vary the probe rate in the range 1 to 6 Mbps with steps of 1 Mbps and develop the Markov model for the SNR measurements obtained at each rate. We summarize our observations next. The SNR thresholds for the models are identical with less than 1% change in the transition probabilities. The maximum difference between the NKLD is less than 2%. Our measurements however indicate that the model parameters do not significantly change with change in the probe rate.

We now explain our observations. There model parameters may be different for different rates for the following two reasons. Firstly the SNR process could itself change as the rate is changed. This is because when the probe packets are transmitted more frequently other users will back off more frequently as well. We now explain why this effect is not pronounced. First note that when the existing aggregate rate on the channel is high, an increase in probe traffic generation rate does not translate to a higher injected probe rate. This is because although the traffic generation rate is increased, the probe traffic injected into the network, in the presence of an already existing user, does not increase beyond 3 Mbps. For higher number of

users when the aggregate existing traffic is more than 4 Mbps, the change in the probe rate injected is even lesser. On the other hand, when the existing aggregate rate in the channel is low, the injection of probe traffic does not significantly disrupt the transmission of other users and hence do not substantially alter the SNR process.

Secondly, even if the process does not change the model statistics can change since the memory is likely to increase as the SNR is measured more frequently with a higher probe rate. However, even for a moderate probe rate of 1 Mbps, the model exhibits high memory (> 0.95). Therefore, the scope for substantial increase in memory with increase in the probe rate is limited. Thus, this effect is not pronounced either.

In this situation, the performance of the model in characterizing the burst process is shown in Fig.19.

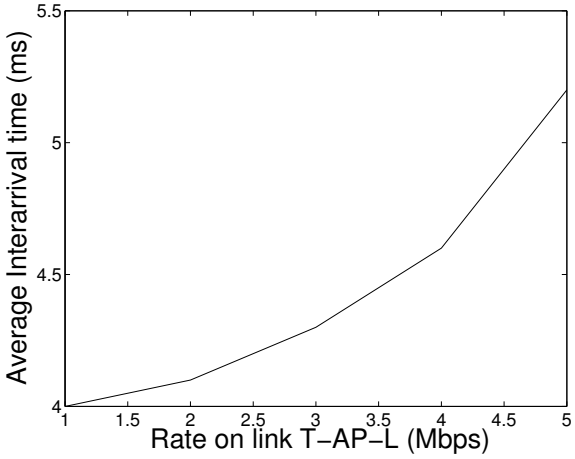

Fig. 17. Variation of Inter-arrival time for AP-C.

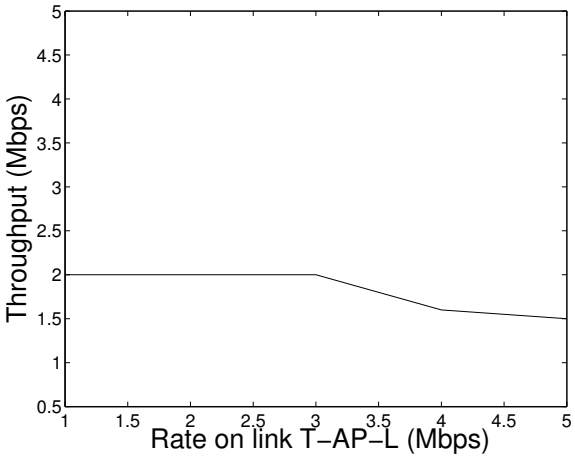

Fig. 18. Variation of throughput for AP-C.

In access points with connected users, sending additional streams will influence the performance observed by the other users. In practice there are two ways to measure the channel characteristics actively using probe packet

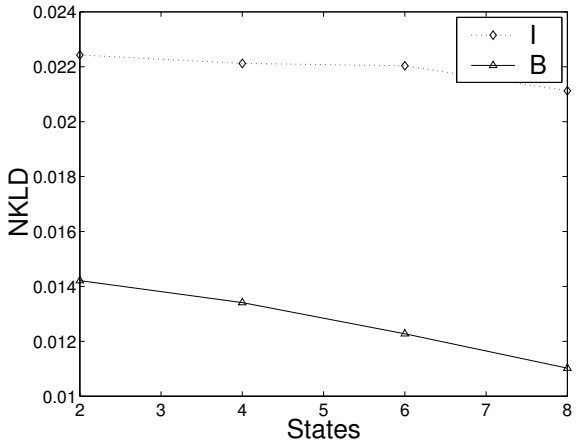

Fig. 19. Measurement from probe packet stream.

streams. We investigate these methods. The first method is to send packets to an AP and measure the channel characteristics from the response packets received from the AP measured by the monitor placed near L. In Fig.16, this corresponds to the case when the node L communicates with the AP and receives ACK packets. In this scenario we vary the traffic rate from 1 to 6 Mbps and develop the Markov model for each probe traffic rate. The transmission rate does not increase beyond 3 Mbps due to the already existing users on the network. The difference in the model parameter values are less than 5% as compared to models developed in Section IV and the divergence measure between the models is close to 0.01. From the perspective of the Markov model, the influence on the channel because of the probe traffic sent by the measuring station is not any different than the effect of other users on the network. The other users could be changing their rates or they could be leaving and joining the network.

Another method is to make the AP send packets to a mobile node using a stream generated from the wired side of the AP. This scenario corresponds to the link T-AP-L in Fig.16. We vary the rate of the traffic sent from the wired side from 1 to 6 Mbps and observe the channel characteristics measured by the monitor M placed near L. The transmission rate does not increase beyond 3 Mbps due to the already existing users on the network. This method of obtaining channel characteristics yields identical results as compared to the case when the traffic destined for an arbitrary user is captured and used to generate characteristics (Fig.20). We now explain the similarities. In Fig.20, we evaluate the difference in the channel model when an additional probe stream is introduced into the network with a certain numbers of existing users as compared to the models derived from passive measurements. We observe that the NKLD increases with the number of users. This can be explained as follows. For few users the

probe traffic can easily be accommodated resulting in little change for traffic patterns of the existing users. When the wireless access point is functioning close to capacity with a large number of users, the effect of adding an additional probe stream is more pronounced. However even in this case with a large number of users, although the overall influence is high, the effect per user is mitigated as can be observed from the slight increase in divergence in Fig.20. The effect of varying the rate is similar to the observations explained previously. We conclude that in common APs, an additional probe traffic does not significantly influence the statistics as captured by the Markov model.

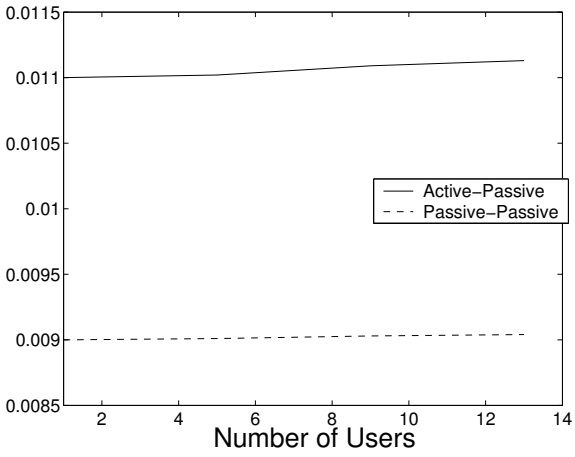

Fig. 20. The influence of the probe packet stream on the channel model. The active-passive shows the divergence between the channel models developed from the probe stream and original passive stream collected from a particular user. The passive-passive shows the divergence between the traffic collected from the user with and without the probe traffic collected within a 5 minutes window.

We now discuss some inferences we make from the model in different 802.11 scenarios.

VII. Inferences from the Model

Based on our measurements, we proceed to identify some features of the model that makes it useful for channel representation. Our work is complementary to efforts in [8] who have conducted measurements primarily from an application layer perspective. They study large-scale characteristics such as application mix, building traffics and mobility patterns while we focus more towards the physical layer aspects and their characterization.

An important parameter of the model is G i.e. the number of states to represent the channel. Specifically the value of G i.e. the number of states needs to be high enough and using $G = 8$ resulted in a good match for all the three types of channels we identified in Section III. High values of G would however increase the computational complexity. Based on model generation from traces collected on different days and times, we notice some broad trends in terms of the 802.11 channel behavior. SNR variation is a reasonably good indicator of the channel quality and packet loss in an 802.11b Access point type network. We obtained the following channel state success probabilities α. For poor channels (SNR $<$ 10dB), α =[0.0000 0.1057 0.1904 0.3019 0.4297 0.5595 0.6782 1.0000] with error rates of 13%. For intermediate channels (SNR 10-20dB), α =[0.0000 0.6785 0.7772 0.8535 0.9083 0.9453 0.9689 1.0000] with error rates of 8%and for good channels (SNR $>$ 25dB) α =[0.0002 0.9980 0.9980 0.9991 0.9996 0.9996 0.9999 1.0000] with error rates of 1.5%. This data can be used to explain the discrepancy between the results reported in prior work. Recall that in [1] and [19] the authors conclude that the two-state Gilbert-Eliot model is not suitable for characterizing packet losses, whereas the authors in [10] claim that two-state models are sufficient for capturing the packet loss process but not the bit losses. Results in [1] and [19] are based on measurements in error-prone channels whereas those in [10] are based on good channels. We note from α for good channels, that using fewer states (e.g. 2) can result in a close match since most of the packet success levels are high as has been observed independently in [10]. However this is not true for intermediate and poor channels since variation in the success probabilities of different states is significant. Therefore, authors in [19], [1] who have studied channels with higher mean burst lengths and error rates, have not observed a good match with a two-state model.

Memory	8-10 a.m	10-12 a.m	12-2 p.m	2-5 p.m
Good	0.8834	0.9327	0.9114	0.9234
Intermediate	0.8815	0.9215	0.9005	0.9107
Poor	0.8231	0.8145	0.8576	0.8435

Fig. 21. Variation in Memory with an 8-state model. The locations for good, intermediate and poor are a classroom, hotspot and a park respectively.

We studied the variation in channel memory i.e. $1 - P_{k,k+1} - P_{k,k-1}$ (Fig.3) with different times of the day and across different days. The channel memory would indicate how rapidly a wireless channel varies. Depending on the variation speed of the channel, algorithms can possibly adjust recomputation to minimize the overhead. The memory of the channels is observed to vary in the range $0.8 - 0.95$. In Fig.21, we tabulate the memory of the 8-state model at different environments with time on a weekday (Monday). Over time (3-4 hours) on the same day, the channel quality varies significantly i.e shifts from

Memory	Monday	Wednesday	Friday	Saturday
8-10 a.m	0.8834	0.8823	0.8814	0.9435
12-2 p.m	0.9114	0.9232	0.9146	0.9431
2-5 p.m	0.9234	0.9217	0.9132	0.9482

Fig. 22. Variation in Memory at classroom AP

Memory	Monday	Wednesday	Friday	Saturday
8-10 a.m	0.8815	0.8807	0.8814	0.9234
12-2 p.m	0.9005	0.8984	0.9034	0.8914
2-5 p.m	0.9107	0.9136	0.9064	0.8642

Fig. 23. Variation in Memory at a T-mobile hotspot

'good' to 'intermediate' and viceversa as the user loads alter. This indicates that number of users and usage patterns plays a major role in determining channel characteristics.

In general a strong similarity between parameters (variation $< 2\%$) was observed in terms of same time at different days at a given location Fig.22,23 and 24. This can be attributed to similar usage patterns. In addition because of recurring user patterns at the same time over different days, models with similar parameters can be utilized again. A memory value of 0.8 is seen in locations with high number of users while very high memory is seen in 'good' channels with very low loss rates. Owing to the high memory of the channel, resource allocation algorithms can possibly make decisions less frequently in order to reduce overheads.

Apart from user patterns different environments also play a major role. In open environments with high delay spread, we observe a loss rate increase ('good' to 'intermediate') with increasing distance that cannot be explained simply based on attenuation of signal levels. Here the loss-rate increases as a result of multipath effects as has been pointed before and the channel attains 'intermediate' loss rates despite low number of users.

Overall, characterizing SNR gives a good insight of the channel characteristics and helps explain behavior that are not directly answered from packet error traces. The proposed model for characterizing SNR captures the channel variation with a reasonable degree of accuracy in terms of SNR and burst length distributions. It can serve as an useful model for analytical scenarios that require tractable models and for computational scenarios.

Memory	Monday	Wednesday	Friday	Saturday
8-10 a.m	0.8231	0.8315	0.8326	0.8444
12-2 p.m	0.8576	0.8424	0.8616	0.8329
2-5 p.m	0.8435	0.8623	0.8458	0.8224

Fig. 24. Variation in Memory at a public park

VIII. Conclusions

We have investigated a model for characterizing SNR variations of a 802.11 channel. The model is simple, analytically tractable and easy to characterize using measured traces. We have discussed an approach to gather the information required to parameterize such a model based on measurements taken from 802.11b access point networks using common hardware. The model is found to represent the packet loss process with reasonable accuracy. The model maintains the birth-death flavor of a two-state model while at the same time improves the performance significantly. Such a model that tracks the temporal variation of SNR can be useful for a variety of resource allocation algorithms and large scale simulations that might require low complexity models.

References

[1] J. Arauz and P. Krishnamurthy. Markov modeling of 802.11 channels. *IEEE Vehicular Technology Conference*, 2003.

[2] Atheros. Atheros wlan chipset. http://www.atheros.com.

[3] A. Balachandran, G. M. Voelker, P.Bahl, and P. V. Rangan. Characterizing user behavior and network performance in a public wireless lan. *SIGMETRICS Perform. Eval. Rev.*, 30(1), 2002.

[4] G. Bianchi. Performance analysis of IEEE 802.11 distributed coordination function. *IEEE Journal on Selected Areas in Communications*, 18(3):535–547, March 2000.

[5] T. M. Cover and J. A. Thomas. *Elements of Information Theory*. John Wiley & Sons Inc., 1991.

[6] E. O. Elliott. Estimates for error rates for codes on burst-noise channels. *Bell Syst. Tech. Journal*, 42(9):1977–1997, 1963.

[7] E. N. Gilbert. Capacity of a burst-noise channel. *Bell Syst. Tech. Journal*, 39(9):1253–1265, 1960.

[8] T. Henderson, D. Kotz, and I. Abyzov. The changing usage of a mature campus-wide wireless network. *Proc. of ACM Mobicom*, 2004.

[9] Intersil. *ISL3874A; Wireless LAN Integrated Medium Access Controller with Baseband Processor with Mini-PCI Features*, August 2001.

[10] S. A. Khayam and H. Radha. Markov-based modeling of wireless local area networks. *Proc. of the 6th ACM workshop on Modeling analysis and simulation of wireless and mobile systems*, 2003.

[11] M. Koes, B.P. Sellner, B. Lisien, G. Gordon, and F. Pfennig. A learning algorithm for localizing people based on wireless signal strength that uses labeled and unlabeled data. *Proc. of IJCAI*, 2003.

[12] Z. Kong, D. H Tsang, B. Bensaou, and D. Gao. Performance analysis of IEEE 802.11e contention-based channel access. *IEEE Journal on Selected Areas in Communications*, 22(10):2095–2106, December 2004.

[13] S. Kullback. *Information theory and statistics*. John Wiley and Sons., New York, 1959.

[14] M. Milner. Netstumbler. http://www.netstumbler.org.

[15] G. T. Nguyen, B. Noble, R. H. Katz, and M. Satyanarayanan. A trace-based approach for modeling wireless channel behavior. *Proc. of the Winter Simulation Conference*, 1996.

[16] H. S. Wang and N. Moayeri. Finite-state markov channel- a useful model for radio communication channels. *IEEE Transactions on Vehicular Technology*, 44(1):163–171, 1995.

[17] WildPackets. Airopeek nx 2.0.5. http://www.wildpackets.com.

[18] A. Willig. A new class of packet- and bit-level models for wireless channels. *IEEE PIMRC*, 2002.

[19] A. Willig, M. Kubisch, C. Hoene, and A. Wolisz. Measurements of a wireless link in an industrial enviroment using an IEEE 802.11-compliant physical layer. *IEEE Transactions on Industrial Electronics*, 49(6):1265–1282, December 2002.

[20] Y. Xu and W. Lee. Exploring spatial correlation for link quality estimation in wireless sensor networks. *IEEE PERCOM*, 2006.

[21] Q. Zhang and S. A. Kassam. Finite-state markov model for rayleigh fading channels. *IEEE Transactions on Communications*, 47(11):1688–1692, 1999.